



## ORIGINAL ARTICLE

# Optimization and ecofriendly synthesis of iron oxide nanoparticles as potential antioxidant

Kuldeep Singh, Dimple Sethi Chopra\*, Dhandeep Singh, Nirmal Singh

Department of Pharmaceutical Sciences and Drug Research, Punjabi University, Patiala 147002, India

Received 16 March 2020; accepted 15 October 2020

Available online 22 October 2020

## KEYWORDS

Iron oxide nanoparticles;  
Box-Behnken design;  
Antioxidants;  
Coriander;  
Green synthesis

**Abstract** The present study involves the use of Box-Behnken design for optimization of the energy-efficient process variables, eco-friendly synthesis of nanoparticles of iron oxide using *Coriandrum sativum* L. (cilantro) leaf extract. The factors, which significantly influenced mean nanoparticle size, surface charge, and size distribution, were the volume of leaf extract, agitation speed, and temperature. The developed model using Box-Behnken design was validated by synthesizing the iron nanoparticles using optimized operational conditions i.e. 10 ml volume of leaf extract, 1500 rpm agitation speed and 30 °C temperature. This resulted in the formation of highly stable iron oxide nanoparticles with mean particle size 161.5 nm and polydispersity index 0.132 with a zeta potential of  $-19.5$  mV. The free radical inhibitory activity of prepared iron oxide nanoparticles was found comparable to ascorbic acid. These results reveal that iron nanoparticles for a biomedical application can be prepared at ambient temperature in an eco-friendly manner.

© 2020 Published by Elsevier B.V. on behalf of King Saud University. This is an open access article under the CC BY-NC-ND license (<http://creativecommons.org/licenses/by-nc-nd/4.0/>).

## 1. Introduction

The iron oxide nanoparticles owing to their distinct physico-chemical properties are one of the most important nanostructure materials in science and technology (Nielsen et al., 2018). These nanoparticles are presently employed for diverse applications; ranging from environmental remediation in earth sciences to biomedicine in life sciences. Iron oxide nanoparticles have many biomedical uses including the treatment of ill-

ness and the drug delivery systems. Disease diagnosis includes applications in MRI (Zhu et al., 2015) and immunoassays; whereas the applications in the drug delivery systems (Tudisco et al., 2015; Majeed et al., 2013) includes hyperthermia (Dorniani et al., 2012), tissue repair and detoxification (Blanco-Andujar et al., 2015). Due to immense importance in the biomedical industry, there is an unmet requirement to develop the iron oxide nanoparticle. Several physicochemical methods like co-precipitation, thermal and electrochemical decomposition, the sonochemical, hydrothermal, microemulsion has used for the synthesis of iron oxide nanoparticles. All these multi-step methods suffer from several limitations like poor control on the size of a particle, requirement of expensive equipment, high temperature, pressure, and energy-intensive processes; which ultimately increase the cost of manufacturing. Furthermore, these iron oxide nanoparticles

\* Corresponding author.

Peer review under responsibility of King Saud University.



Production and hosting by Elsevier

have to be coated with suitable agents to prevent their agglomeration. Hence, green synthesis becomes the method of choice for the preparation of iron oxide nanoparticles due to easy processing, low economic constraints and high efficiency. Further, there is no requirement for high temperature and pressure and thus minimal energy and cost; requiring a single step synthetic process (Kim et al., 2010). The bio-reductant present in the plant extract serves the dual purpose of reducing agent in synthesis and stabilizing agent in preventing agglomeration (Hoag et al., 2009). These bio reductants are phytochemicals such as amino acids, carbohydrates, flavonoids, and polyphenols (Njagi et al., 2010). Several studies have reported the synthesis of iron oxide nanoparticles using plant extract but none based on optimizing the reaction conditions for iron oxide nanoparticles preparation (Nadagouda et al., 2010).

Coriander (*Coriandrum sativum* L.) is one of the oldest herbs used in the Umbelliferae (Apiaceae) family for more than 3000 years (Ebers papyrus, 1550 BCE), both for medicinal and culinary purposes. (Ishikawa et al., 2003). Due to its attractive green color and fragrance, the green leaves are used as fresh herbs, in salads and sauces (Kamat et al., 2003). The coriander leaves are a rich source of natural antioxidants like kaempferol ( $3.49 \pm 0.40\%$ ), p-Coumaric acid ( $4.39 \pm 0.55\%$ ) 4'-O mequercetin quercetin ( $5.62 \pm 0.66\%$ ), 3'-O-mesquercetin ( $9.19 \pm 0.24\%$ ), acetin ( $3.91 \pm 0.45\%$ ), *trans*-ferulic acid ( $11.07 \pm 0.66\%$ ) and vanillic acid ( $7.51 \pm 0.55\%$ ) (Nambiar et al., 2010). The present study involves the preparation of iron oxide nanoparticles from the aqueous extract of *Coriandrum sativum* leaf and understanding the influence of reaction conditions like the volume of leaf extracts (10%w/v), agitation speed, and temperature. The minimum concentration of plant extracts required for the synthesis of iron oxide nanoparticles was selected based on FTIR of prepared iron oxide nanoparticles. A combination of mathematical and statistical methods, Box-Behnken design was applied to determine optimal experimental conditions for reproducible synthesis of monodisperse iron oxide nanoparticles from *Coriandrum sativum* leaf extract. Iron oxide nanoparticles thus prepared using the coriander leaf extract can be used as a potential antioxidant, antimicrobial and anticancer agent (Rodger et al., 2015).

## 2. Materials and methods

Ferrous sulfate heptahydrate, AR was purchased from Himedia Pvt Laboratories (Mumbai, India). The *coriandrum sativum* L. An annual herb belonging to the family Apiaceae (Umbelliferae) commonly known as coriander. For further research, fresh coriander leaves were collected from the local market (January-March 2019).

### 2.1. Preparation of coriander leaf extract

Fresh leaves from *Coriandrum sativum* L. (cilantro) have been collected and washed with deionized water. The aqueous leaf extract was prepared by taking in a 250 ml beaker with 100 ml of deionized water and 10 gm of coriander leaves was cut into small parts. The solution was boiled in the water-bath at 30 °C for 15 min and plant leaf extract then was cooled and filtered with Whatman No.1 filter paper and stored at 5 °C in a clean sealed flask for further studies.

### 2.2. Biosynthesis of iron oxide nanoparticles

Nanoparticles of iron oxide have been prepared by adding coriander leaf extract dropwise to 0.01 mM FeSO<sub>4</sub> in a 100 ml conical flask with constant agitation speed at 1500 rpm. The immediate presence of black colour suggested a reduction of Fe<sup>+2</sup> ions to zero-valent iron (Fig. 1). A magnetic stirrer was used to agitate the reaction mixture at 30 °C for 15 min (Hariani et al., 2013). The prepared iron oxide nanoparticles were then separated at 15,000 rpm for 20 min by centrifugation. The pellet was washed with triple distilled water and purified by repeated centrifugation. The iron oxide nanoparticles were freeze-dried for 24 h at -78 °C with a pressure of 10 Pa. The reduction of Fe<sup>+2</sup> to zero-valent iron was confirmed by the measurement of the UV spectra in the 200–800 nm range.

### 2.3. In-vitro antioxidant activity

The iron oxide nanoparticles the antioxidant study was conducted using the free radical assay 1,1-diphenyl-2-picrylhydrazyl radicals (DPPH), as defined in (Blois, 1958). Different concentrations of iron oxide nanoparticles (50, 100, 150, 200 and 250 µg / ml) were mixed with 2 ml of freshly prepared DPPH solution (1 mM in ethanol) and mixed thoroughly. The resulting solution was then incubated for 30 min in a dark place at 25 °C. The absorbance was taken at 517 nm using UV-visible spectrophotometer using ethanolic ascorbic acid as a reference standard. DPPH (all reagent except sample) was used as a control solution, and ethanol was used as a blank. The DPPH free radical scavenging activity expressed as the percentage of inhibition, which was calculated using the following formula:

$$(\%) \text{ inhibition} = \{(D_0 - D_1) / D_0\} \times 100 \quad (1)$$

Where D<sub>0</sub> represents the absorbance of the control, D<sub>1</sub> is the absorption of the sample. The IC<sub>50</sub> value (µg / mL) was determined, a minimum sample concentration that inhibits 50% radical DPPH.

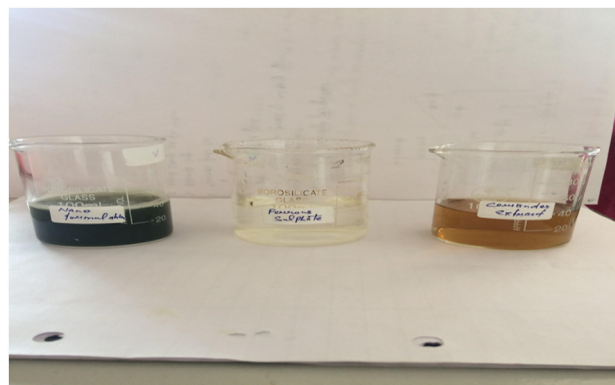


**Fig. 1** (a) Synthesized iron oxide nanoparticles (b) 0.01 M ferrous sulphate and (c) Coriander leaf extract.

**Table 1** Box-Behnken design containing dependent and independent factors and their outcomes.

Run	X	X	X	Response	Response	Response
	1	2	3	1	2	3
	plant Leaf extract (ml)	Agitation speed (RPM)	Temperature ( $^{\circ}$ C)	Particle Size (nm)	Zeta Potential (mV)	PDI
1	30.00	1500.00	30.00	654 $\pm$ 2.05	-7.83 $\pm$ 2.94	0.273 $\pm$ 1.45
2	50.00	1000.00	45.00	987 $\pm$ 2.45	-6.56 $\pm$ 3.15	0.394 $\pm$ 1.09
3	10.00	1500.00	45.00	142 $\pm$ 2.67	-20.65 $\pm$ 1.34	0.095 $\pm$ 1.25
4	50.00	1250.00	65.00	783 $\pm$ 2.12	-9.13 $\pm$ 1.67	0.352 $\pm$ 1.19
5	30.00	1250.00	45.00	655 $\pm$ 1.89	-5.33 $\pm$ 1.86	0.262 $\pm$ 1.16
6	50.00	1250.00	30.00	854 $\pm$ 1.67	-4.37 $\pm$ 2.45	0.473 $\pm$ 1.02
7	30.00	1250.00	45.00	765 $\pm$ 1.98	-8.24 $\pm$ 2.67	0.357 $\pm$ 1.02
8	30.00	1250.00	45.00	728 $\pm$ 1.93	-9.89 $\pm$ 2.74	0.314 $\pm$ 0.98
9	30.00	1000.00	60.00	742 $\pm$ 2.12	-5.67 $\pm$ 2.56	0.352 $\pm$ 1.12
10	10.00	1250.00	30.00	161 $\pm$ 2.	-18.65 $\pm$ 2.89	0.152 $\pm$ 1.26
11	30.00	1250.00	45.00	663 $\pm$ 2.76	-6.93 $\pm$ 2.95	0.253 $\pm$ 1.12
12	10.00	1000.00	45.00	195 $\pm$ 2.84	-1638 $\pm$ 3.10	0.131 $\pm$ 1.31
13	10.00	1250.00	60.00	173 $\pm$ 2.89	-16.97 $\pm$ 3.56	0.121 $\pm$ 1.08
14	30.00	1500.00	60.00	535 $\pm$ 2.76	-7.64 $\pm$ 3.26	0.273 $\pm$ 1.14
15	30.00	1000.00	30.00	547 $\pm$ 2.67	-9.87 $\pm$ 3.03	0.168 $\pm$ 1.76
16	50.00	1500.00	45.00	954. $\pm$ 3.18	-7.56 $\pm$ 3.41	0.431 $\pm$ 1.17
17	50.00	1250.00	45.00	663 $\pm$ 2.18	-6.93 $\pm$ 3.41	0.253 $\pm$ 1.13

**Table 2** Model fitting and statistical analysis.

Responses	Model	C.V%	<i>p</i> -value	PRESS	R-squared	Adjusted R-squared	Predicted R-squared	Adequate precision
Particle Size	Quadratic	9.61	<0.0001	2.331E+05	0.9807	0.9559	0.8068	19.1025
Zeta Potential	Quadratic	17.97	0.0013	188.02	0.9445	0.8731	0.5305	10.7398
PDI	Liner	19.36	<0.0001	0.0673	0.8195	0.7778	0.6676	11.5012

**Table 3** Analysis of variance (ANOVA) calculated Quadratic model for response of Particle Size.

Source	Sum of squares	D.F	Mean	F	P-Value	Significance
			Square	Value	Prob > F	
Model	1.183E+06	9	1.315E+05	39.56	<0.0001	Significance
X <sub>1</sub>	1.056E+06	1	1.056E+06	317.84	<0.0001	
X <sub>2</sub>	4324.50	1	4324.50	1.30	0.2915	
X <sub>3</sub>	36.13	1	36.13	0.0109	0.9199	
X <sub>1</sub> X <sub>2</sub>	100.00	1	100.00	0.0301	0.8672	
X <sub>1</sub> X <sub>3</sub>	1722.25	1	1722.25	0.5182		0.4949
X <sub>2</sub> X <sub>3</sub>	24649.00	1	24649.00	7.42	0.0296	
X <sub>1</sub> <sup>2</sup>		66872.84	1	66872.84	20.12	0.0028
X <sub>2</sub> <sup>2</sup>	2.21	1	2.21	0.0007	0.9801	
X <sub>3</sub> <sup>2</sup>	24336.00	1		24336.00	7.32	0.0304
Residual	23264.55	7	3323.51			
Lack of fit	13627.75	3	4542.58	1.89	0.2731	Non-significance
Pure error	9636.80	4	2409.20			
Cor total	1.207E+06	16				

#### 2.4. Statistical optimization using design of experiments (DoE)

Box Behnken Design using Design Expert statistical software (version 11.0) were designed to optimize the process parameters used during the synthesis of iron oxide nanoparticles.

According to the DoE, the 3-factor 3-level Box Behnken design generated 17 experimental runs containing three independent variable and corresponding responses. The concentration of leaf extract (X1), agitation speed (X2) and temperature (X3) were selected as independent variables and particle size (Y1), zeta potential (Y2) and PDI (Y3) were taken as evalua-

**Table 4** Analysis of variance (ANOVA) calculated Quadratic model for response of Zeta Potential.

Source	Sum of Squares	D.F	Mean	F	P-Value	
			Square	Value	Prob > F	
Model	378.24	9	42.03	13.23	0.0013	Significance
X <sub>1</sub>	253.46	1	253.46	79.81	< 0.0001	
X <sub>2</sub>	3.38	1	3.38	1.06	0.3365	
X <sub>3</sub>	0.2145	1	0.2145	0.0675	0.8024	
X <sub>1</sub> X <sub>2</sub>	2.67	1	2.67	0.8418	0.3894	
X <sub>1</sub> X <sub>3</sub>	10.37	1	10.37	3.26	0.1137	
X <sub>2</sub> X <sub>3</sub>	4.02	1	4.02	1.27	0.2976	
X <sub>1</sub> <sup>2</sup>	102.15	1	102.15	32.17	0.0008	
X <sub>2</sub> <sup>2</sup>	0.6670	1	0.0070	0.2100	0.6606	
X <sub>3</sub> <sup>2</sup>	0.0505	1	0.0505	0.0159	0.9032	
Residual	22.23	7	3.18			
Lack of fit	10.62	3	3.54	1.22	0.4113	Non-significance
Pure error	11.61	4	2.90			
Cor total	400.47	16				

**Table 5** Analysis of variance (ANOVA) calculated Liner model for response of PDI.

Source	Sum of squares	D.F	Mean	F	P-Value	
			Square	Value	Prob > F	
Model	0.1658	3	0.0553	19.67	< 0.0001	Significance
X <sub>1</sub>	0.1656	1	0.1656	58.93	< 0.0001	
X <sub>2</sub>	0.0001	1	0.0001	0.0324		0.8599
X <sub>3</sub>	0.0001	1	0.0001	0.0455		0.8343
Residual	0.0365	13	0.0028			
Lack to fit	0.0280	9	0.0031	1.45	0.3823	Non-Significance
Pure Error		0.0086	4	0.0021		
Cor Total	0.2024					

tive responses. Statistical and diagnostic tests were they carried out to determine the adequate mathematical model for analysis using multi regression statistical analysis (MRSA). To demonstrate the interaction between independent and dependent variables, perturbation design and 3-D surface designs were plotted. Analysis of Variance (ANOVA) and polynomial equations were performed for evaluation of significance level of a mathematical model.

## 2.5. Characterization of synthesized iron oxide nanoparticles

### 2.5.1. Fourier transformed infrared spectroscopy (FT-IR)

The chemical interactions of test samples were carried out in Fourier Transform Infrared Spectrophotometer (FTIR) (Bruker, Germany). The synthesized plant-extract iron oxide nanoparticles were mixed with potassium bromide (KBr) pellets. For each measurement, approximately 32 running scans were collected with a resolution of 4 cm<sup>-1</sup> at a finger print range of 4000–500 cm<sup>-1</sup> (Das et al., 2014).

### 2.5.2. Energy dispersive X-Ray spectroscopy (EDXS)

The study of the energy-dispersive X-ray spectroscopy (EDXS) was performed in well-calibrated EDXS instrument (Bruker, Germany) fitted working at a 200 kV acceleration voltage. The solid samples were prepared by drying a drop of the

diluted distribution of the iron oxide nanoparticles on a clear carbon film in a copper grid (Prasad et al., 2014).

### 2.5.3. Field emission-scanning electron microscopy (FE-SEM)

The study of Field Emission-Scanning Electron Microscope carried out using Hitachi S-4800 (Tokyo, Japan). The conditions used were: extra high voltage 0.5–30 kV, working distance 7000 um, (Zhuang et al., 2014) secondary electrons display mode, high vacuum, and room temperature (25 °C).

### 2.5.4. Dynamic light scattering (DLS) studies

The particle size of the different formulations was calculated by the Malvern particle size analyzer (Malvern, UK), using the DLS phenomenon theory. Aliquots were prepared by dissolving 10 mg of iron oxide nanoparticles into 10 ml of deionized water. Further dilutions were executed at 1:100 v/v fold and mean particle size was determined at a scattering angle of -173° at backscattering mode (Turakhia et al., 2018).

### 2.5.5. Zeta potential and electrophoretic studies

The Zeta potential of developed formulations was determined using Malvern Zeta sizer (Malvern, UK). The samples were diluted in 1:100 v/v fold and were put in transparent (10 × 10 mm) disposable cuvettes. The samples were tested

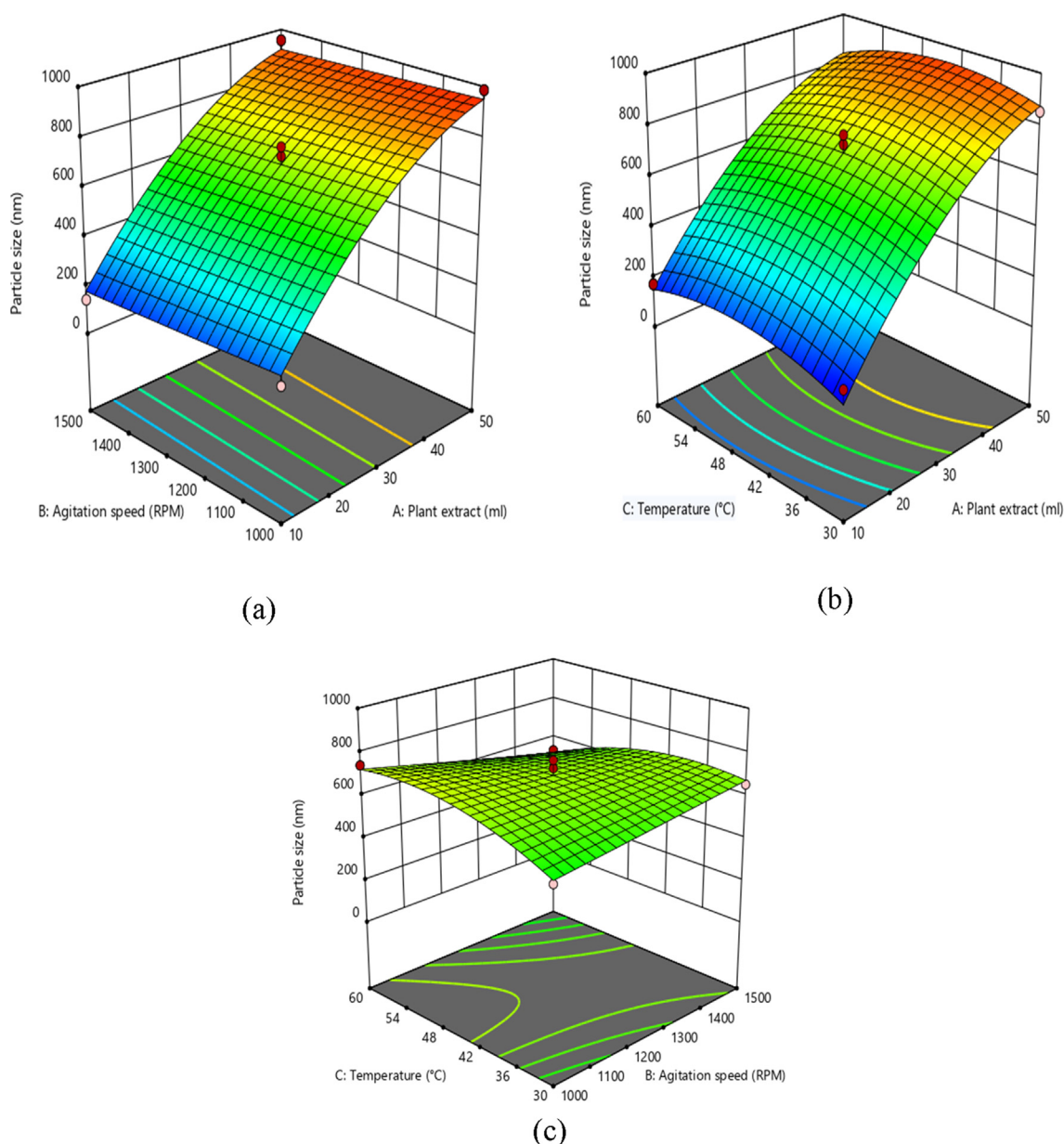


**Fig. 2** 3D response surface graph showing the effect on independent variables on mean particle size.

for zeta potential by running the samples at 10 zeta runs in a backscattering mode and at a temperature of 25 °C (Turakhia et al., 2017).

### 3. Results and discussion

#### 3.1. Design of experiments (DoE)

The entire design summary containing observations gathered from dependent and independent variables are showing in Table 1.

Statistical process optimization of the development of iron oxide nanoparticles were obtained from Surface Response Methodology (RSM). Our objectives of RSM was to identify the maximum prominent interactions between important parameters to generate the minimum sized iron oxide nanoparticles with optimum uniformity and stability. From these

investigations of particle size (Y1), zeta potential (Y2) and PDI (Y3) were found to lie in the range of 161.5 nm, −19.5 mV and 0.132 respectively. The selection of the mathematical model was based on several statistical parameters in Design-Expert Software. The uniformity in sequential p-value and lack of fit p values at 99% confidence intervals ( $p < 0.001$ ) indicated the statistical significance and adequacy of the model terms. The adjusted and predicted R<sup>2</sup> values of all the response showed an equal correlation of  $> 0.997$  suggesting the satisfactory quality of statistical analysis (Table 2). For analysis of interaction effects, the polynomial analysis says that positive values are synergistic outcome on the response and the negative values represent an antagonistic outcome on the response (Sood and Chopra, 2018). After statistical evaluation of responses, the Linear and Quadratic model were selected for Y1, Y2 and Y3 respectively. The polynomial equations in terms of coded factors are depicted in (2), (3) and (4).

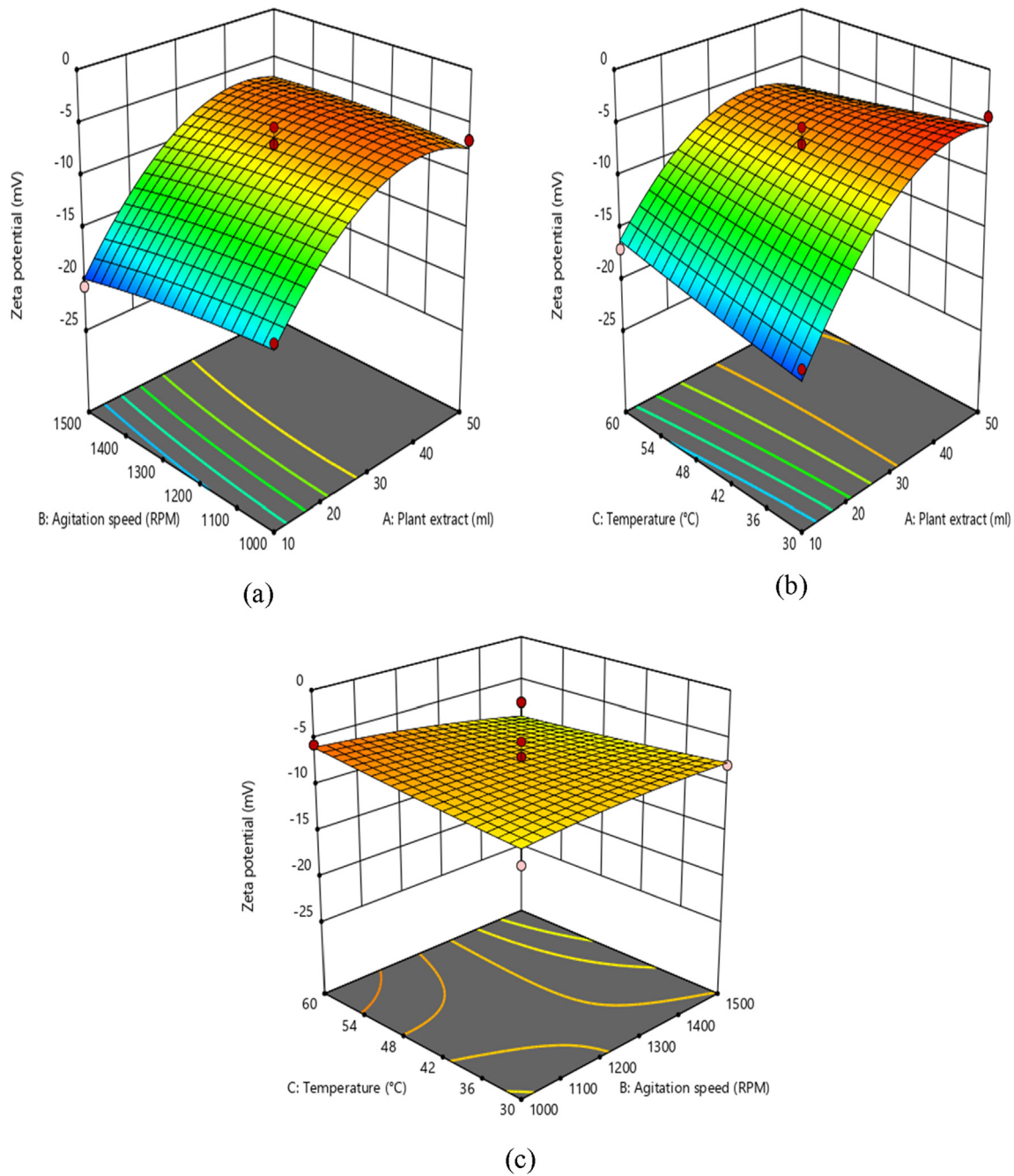


**Fig. 3** 3D response surface graph showing the effect on independent variables on zeta potential.

$$\begin{aligned}
 \text{Particle Size} = & +38.93500 X_1 + 0.790000 X_2 + 58.79333 X_3 \\
 & +0.001000 X_1X_2 - 0.069167 X_1X_3 \\
 & -0.020933 X_2X_3 \\
 & -0.315062 X_1^2 + 0.000012 X_2^2 - 0.337889 X_3^2 \\
 \text{Model} = & \text{Quadratic}; (R^2 = 0.9807)
 \end{aligned}
 \tag{2}$$

$$\begin{aligned}
 \text{Zeta Potential (mV)} = & +1.05739X_1 + 0.020445X_2 + 0.462283X_3 \\
 & +0.000164X_1X_2 - 0.005367X_1X_3 - 0.000267X_2X_3 \\
 & -0.012314 X_1^2 - 6.36800E - 06X_2^2 + 0.000487X_3^2 \\
 \text{Model} = & \text{Quadratic}; (R^2 = 0.9445)
 \end{aligned}
 \tag{3}$$

$$\begin{aligned}
 PDI = & +0.007194X_1 + 0.000014X_2 + 0.000267X_3 \\
 \text{Model} = & \text{Liner}; (R^2 = 0.8195)
 \end{aligned}
 \tag{4}$$

The significance and appropriateness of the model were tested using Fischer statistical analysis through ANOVA, as illustrated in Tables 3–5. The surface plots of 3D responses reflect the interaction between variables and describe each parameter’s optimal condition for the development of desired iron oxide nanoparticles, as illustrated in Figs. 2–4. The average effect of the variables showed that that X<sub>1</sub> (10–50 ml) increased the particle size of iron oxide nanoparticles, while X<sub>2</sub> (1000–1500 rpm) decreased iron nano size.

In addition, the decrease in X<sub>1</sub> extract leads to the rise in zeta potential, with the minimum PDI, which is a measure of

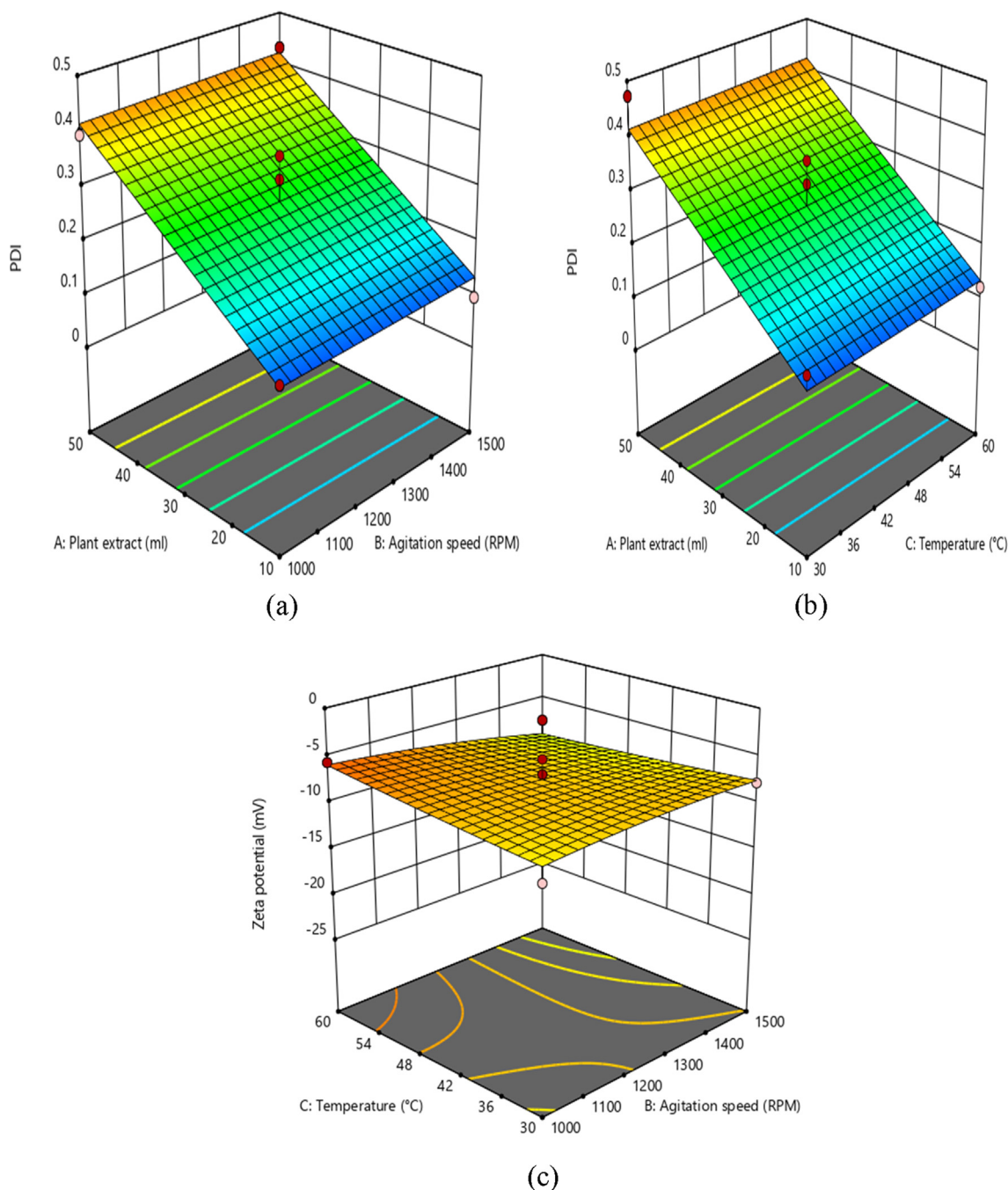


**Fig. 4** 3D response surface graph showing the effect on independent variables on PDI.

the homogeneity in solution particles. Furthermore, the perturbation plot in Fig. 5 also clearly shows correlations between the variables.

### 3.2. Validation of data by numerical optimization

Innovative research was shown in accordance with suggested parameters to validate the optimization, which combines all the responses in one measurement also offers a view of predicting the optimal degree of independent variables, based on the correlation plots and approach to desirability as seen in Fig. 6. The prepared formulations were evaluated and the

data were found to fit well with the predicted model values with < 5% error as shown in Table 6. However, the optimized batch having minimum particle size of 157.3 nm has a minimum PDI of 0.129 and highest zeta potential of  $-20.5$  mV was selected. The optimal desirability approach was respectively predicted by solving the model at the optimum agitation speed of 1500 rpm, temperature 300 °C and plant leaf extract of 10 ml. For further studies, thus optimized formulation was selected with optimum desirability. Therefore, to carry out further experiments, the optimized concentration of iron oxide nanoparticles was lyophilized.

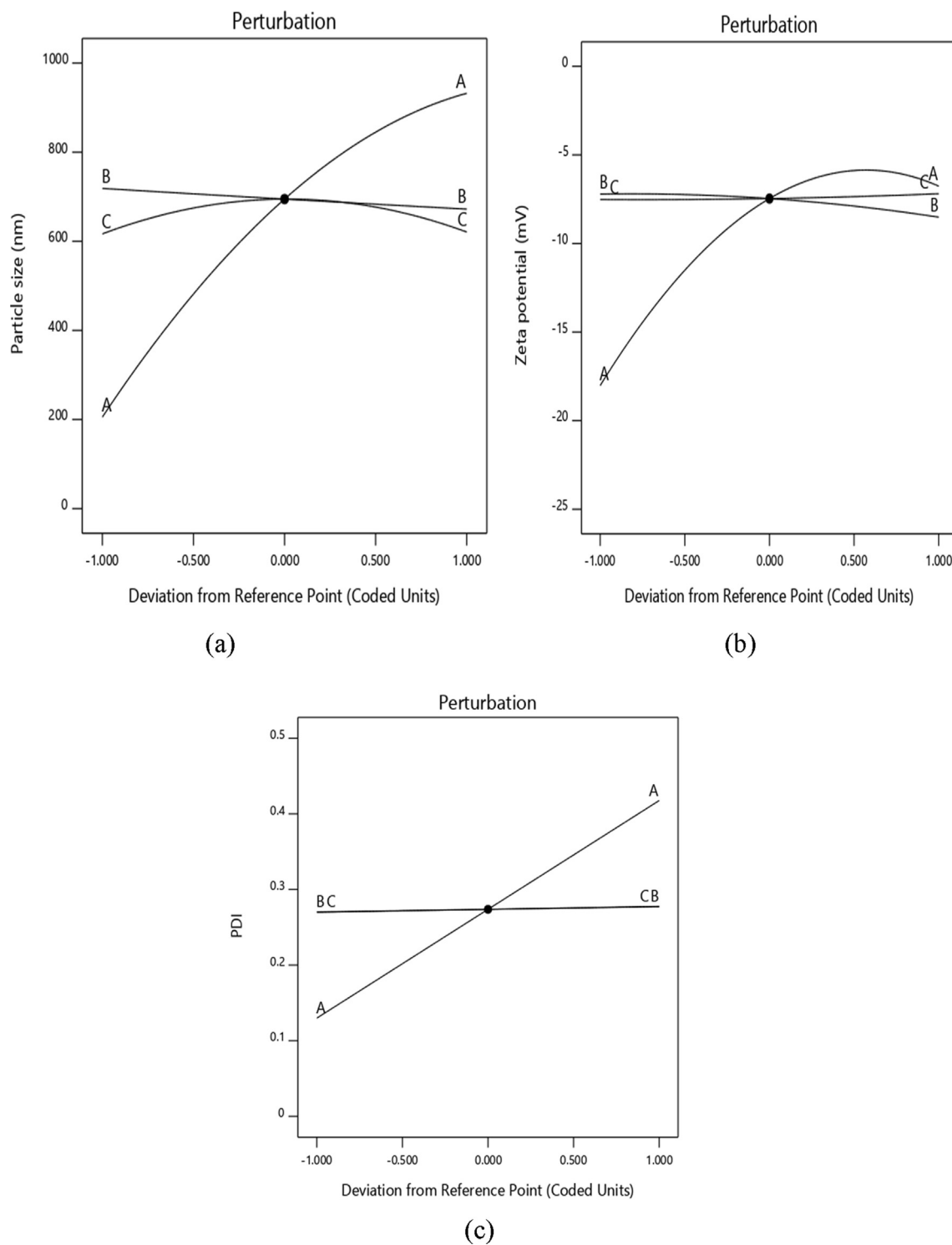


**Fig. 5** Perturbation plot of showing the effect of (a) particle size (nm) (b) zeta potential (mV) (c) PDI.

3.3. Determination of antioxidant capacity

3.3.1. 2, 2-diphenyl-1-picrylhydrazyl (DPPH) activity

The free radical inhibitory activity of different concentrations of iron oxide nanoparticles (50–250 µg) on DPPH ranged from 32.54 to 84.28%, whereas ascorbic acid ranged from 28.25 to 81.41. The findings showed stronger antioxidant

ability compared to DPPH radical scavenging activity with standardized ascorbic acid. The IC<sub>50</sub> value of iron oxide nanoparticles on DPPH radical was obtained were as 86.68 µg/ml, which was compared with standard ascorbic acid (IC<sub>50</sub> = 107 µg/ml). Some studies reported DPPH radical reduce the hydrogen donating ability of phenolics and flavonoids (Fig. 7).

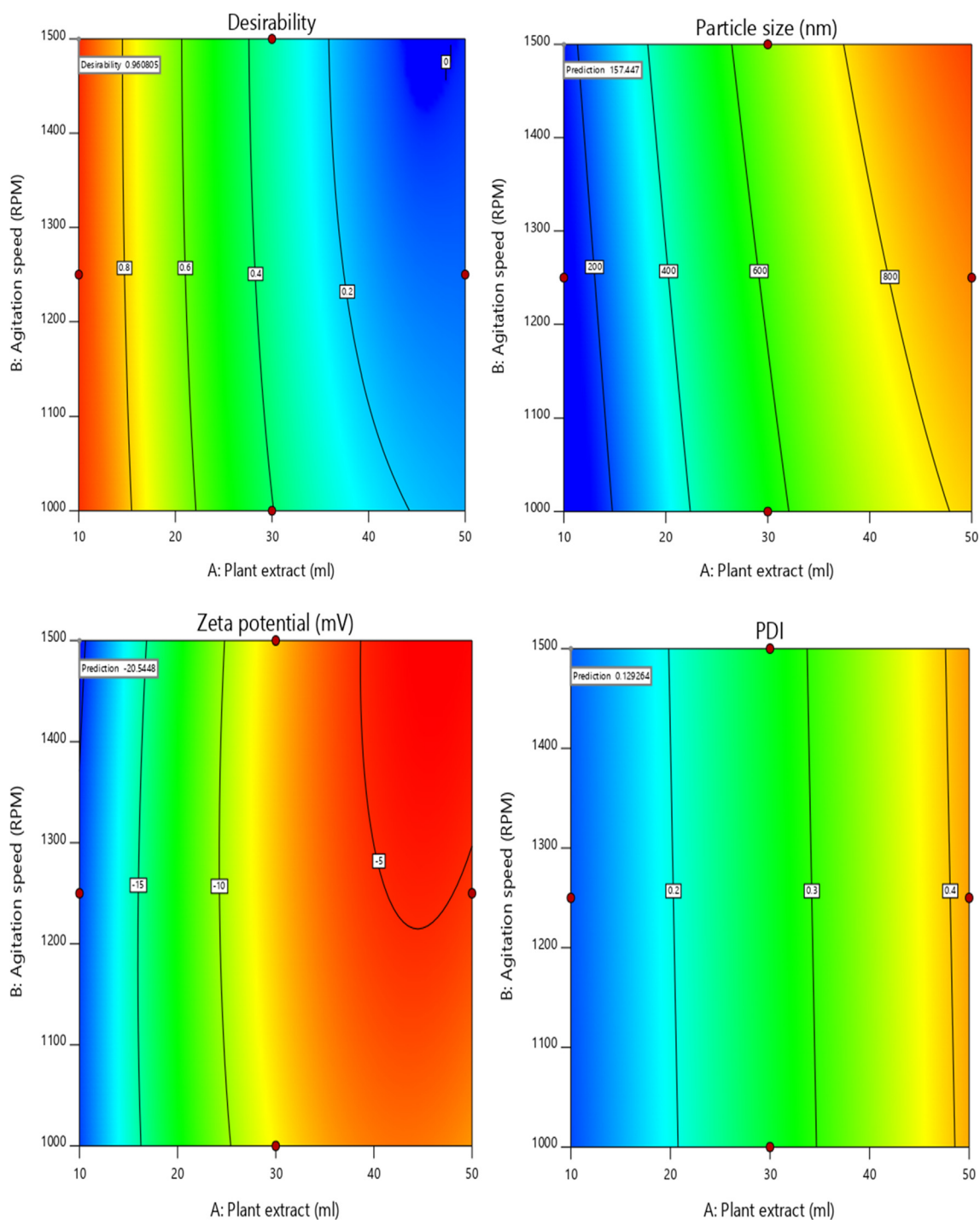


**Fig. 6** Contour plots representing desirability of optimized formulation.

### 3.4. Ultraviolet–visible analysis

UV–visible Spectroscopy is an analytical technique, which concerned the measurement of electromagnetic radiation absorption (Mulvaney, 1996). UV–visible spectral analysis was initiated at a wavelength of 200–800 nm to study the absorption spectrum of green synthesized iron oxide nanoparticles and absorption peaks were observed in 210–330 nm

regions because of surface excitation Plasmon vibrations in iron oxide nanoparticles. (Fig. 8).

### 3.5. Particle size and PDI analysis

Mean particle size is a significant parameter for preconcentration nanoformulations, as the particle of the nanoscale favours increased product absorption and dissolution. The mean parti-

**Table 6** Statistical optimization of biosynthesized iron oxide nanoparticles.

Formulations		A	B	C
Plant leaf extract, Agitation speed		10.00	13.00	17.00
Temperature		1499	1250	1000
		30.00	30.00	30.00
Particle Size	Predicted	157.3	246.2	350.2
	Observed	161.5	256.4	361.3
	%Variation	2.60%	3.97%	3.07%
Zeta Potential	Predicted	-20.5	-17.4	-12.8
	Observed	-19.5	-18.1	-14.3
	%Variation	4.87%	3.8%	10.4%
PDI	Predicted	0.129	0.13	0.21
	Observed	0.132	0.14	0.22
	%Variation	2.27%	7.14%	4.54%
Desirability		0.960	0.936	0.983

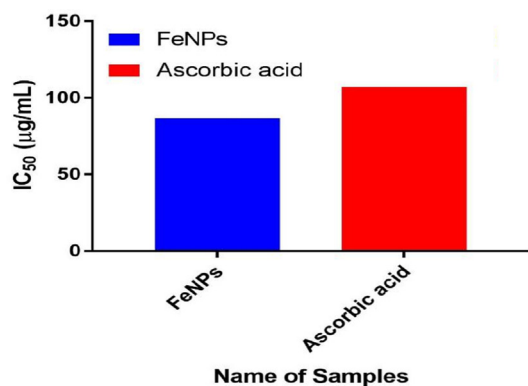


**Fig. 7** Determination of IC<sub>50</sub> of iron oxide nanoparticles and standard ascorbic acid.

cle size of the iron oxide nanoparticles was 161.5 nm due to the increased interfacial surface area. The Polydispersity Index (PDI) has also used to attain information on the size distribution and homogeneity of nanoformulations (Fig. 9a).

### 3.6. Zeta potential analysis

Zeta potential provides information on nanoformulations stability, and the negative value suggests a decreased particle aggregation in the continuous phase (Shi et al., 2012). The possible zeta potential value was found to be -19.5 mV, which indicate moderately stable of the nanoparticles (Fig. 9b) (Bhattacharjee, 2016). The negative value of iron oxide nanoparticles corroborates conjugation of polyphenolic compounds kaempherol, 4'- O mequercetin quercetin, 3'- O mesquercetin, acetin, vanillic acid and *trans*-ferulic acid on to the surface of iron oxide nanoparticles (Igwe and Nwamezie, 2018).

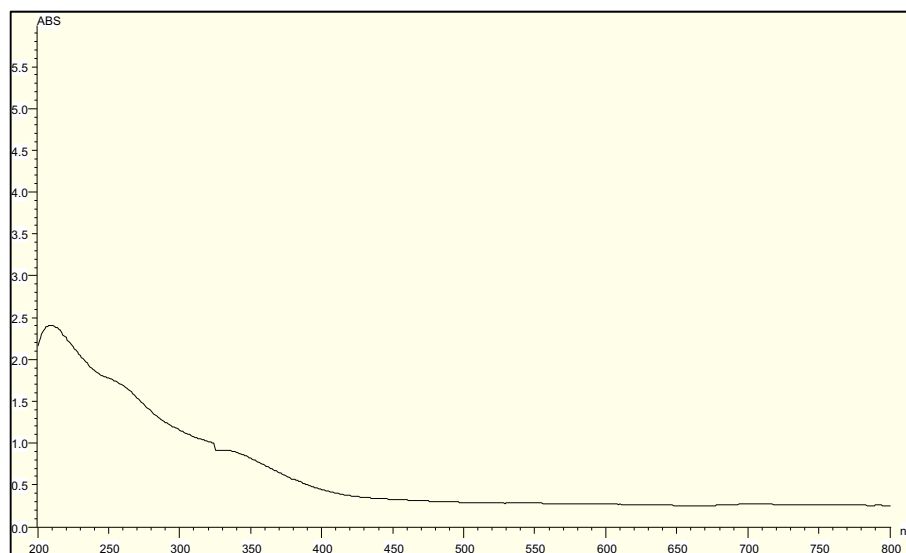


**Fig. 8** UV-visible spectroscopy of iron oxide nanoparticles.

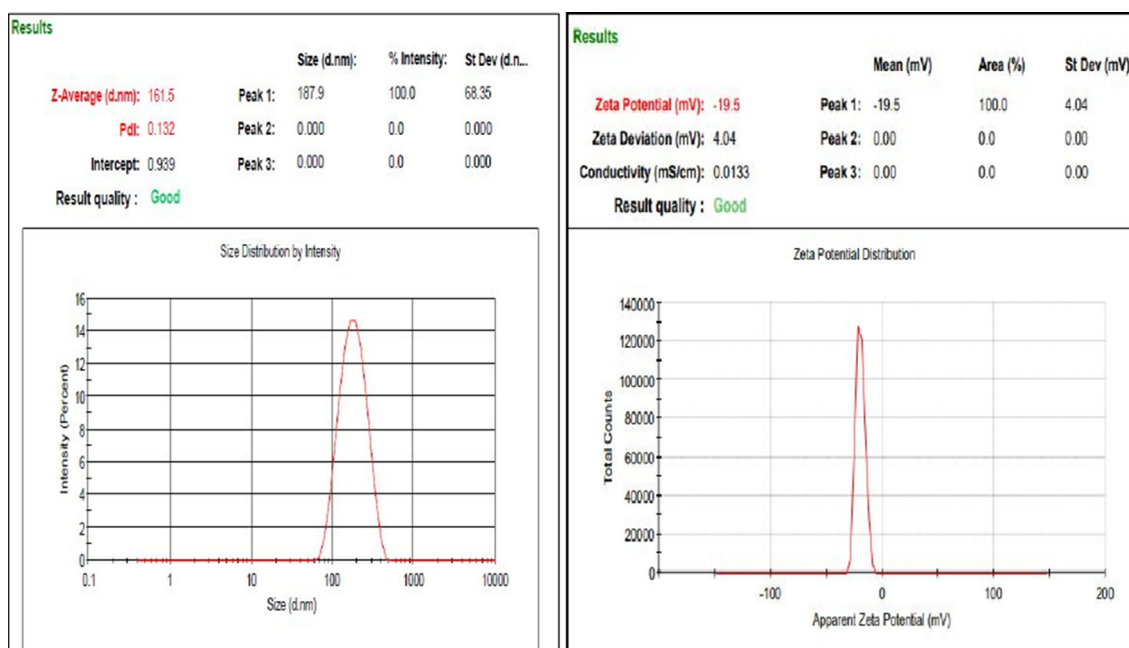


**Fig. 9** (a) Mean particle size and (b) Zeta potential of optimized iron oxide nanoparticles.

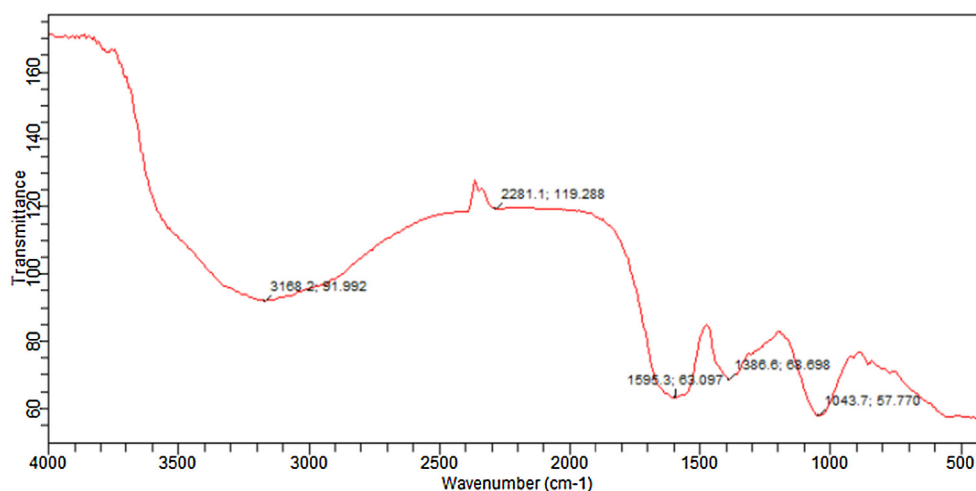


**Fig. 10** FTIR spectra of optimized iron oxide nanoparticles.

### 3.7. Fourier transformed spectroscopy

FTIR spectra of biosynthesized iron oxide nanoparticles were reported to find the capping and successful stabilization of nanoparticles by biomolecules in coriander leaf extract (Wang et al. 2014). Fig. 10 showed the FTIR spectrum of synthesized iron oxide nanoparticles with coriander leaf extract. The strong band near 3168 cm<sup>-1</sup> indicate the presence of aromatic CH stretching and broad-band at 3200–3600 cm<sup>-1</sup> indicate OH stretching which may due to presence of the phenolic compound. Hence, the coating of iron oxide nanoparticles with coriander extract can be inferred from this data

(Mahdavi et al., 2013). This is in correlation with the presence of phenolic compounds in coriander extract.

### 3.8. EDXS analysis

The study of iron oxide nanoparticles by Energy Dispersive X-ray Spectroscopic (EDXS) is shown in Fig. 11, and their elemental compositions are outlined in Table 7. The presence of an extreme peak of Fe, which confirms iron oxide nanoparticles formation. The oxygen signals must originate from FeSO<sub>4</sub> and coriander extract precursors respectively, Used in iron oxide nanoparticles synthesis (Shahwan et al., 2011). The Car-

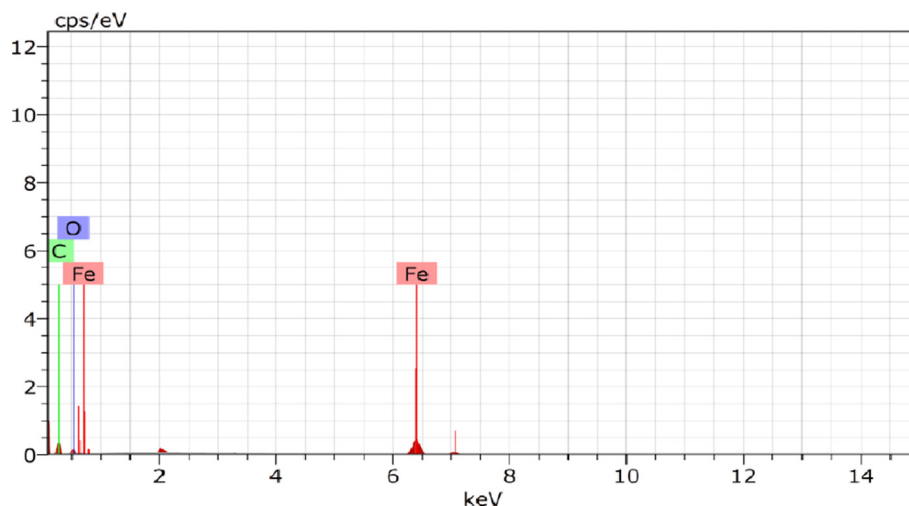


**Fig. 11** Energy-dispersive spectrometry of optimized iron oxide nanoparticles.

**Table 7** Elemental composition of iron oxide nanoparticles.

Elements	Iron oxide nanoparticles	
	Weight%	Atomic%
Iron	67.07 ± 0.03	31.40 ± 0.21
Carbon	27.24 ± 0.05	69.30 ± 1.07
Oxygen	5.79 ± 0.24	9.29 ± 1.35

Each value stands for the mean of three experiments ± S.E.

bon peaks appear because of the use of carbon film during EDXS measurement.

### 3.9. FE-SEM analysis

The FE-SEM images of synthesized lyophilized iron oxide nanoparticles in the current research are showing with different magnification scale 20,000× and 15,000× in Fig. 12. The biosynthesized nanoparticles were spherical in shape with

polydispersity (Gupta and Gupta, 2005). These results show that the significance of coriander leaf extract in the synthesis of iron oxide nanoparticles but the synthesized of nanoparticles show some agglomeration that was indicated by spherical shape and non-uniform particles size with the different void spaces.

### 4. Conclusion

Iron oxide nanoparticles were efficiently prepared using *Coriandrum sativum* L. (cilantro) leaf extract. The optimization design predicted the values of mean particle size of iron oxide nanoparticles as 157.3 nm, polydispersity index as 0.129 and zeta potential as -20.5 mV. The optimized batch of iron oxide nanoparticles thus prepared exhibited mean particle size of iron oxide nanoparticles as 161.5 nm, polydispersity index as 0.132 and zeta potential as -19.5 mV. The volume of plant extract (10% w/v) highly influenced the mean particle size of iron oxide nanoparticles. The iron oxide nanoparticles thus produced were monodisperse with a very high value of zeta potential, indicating maximum repulsion and minimum

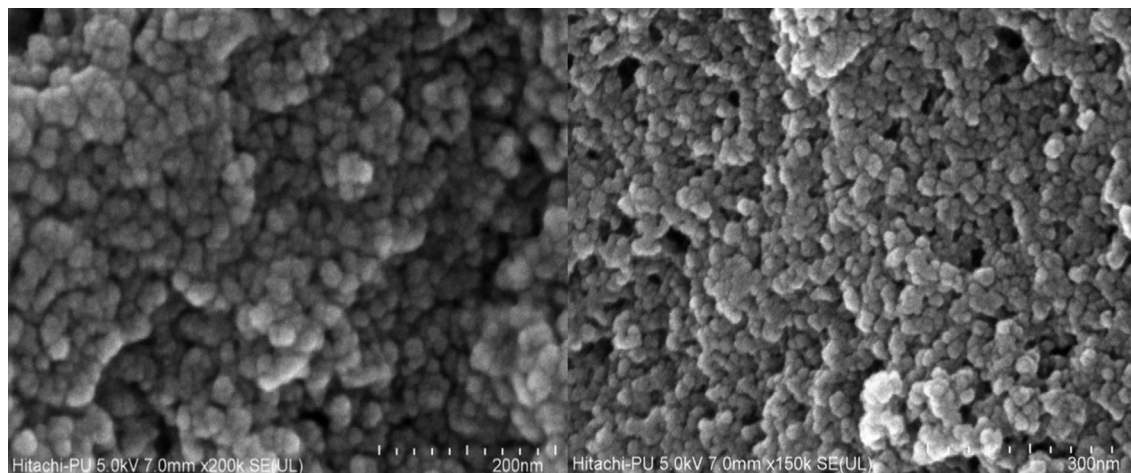


**Fig. 12** Field emission-scanning electron microscope images of iron oxide nanoparticles.

agglomeration between prepared iron oxide nanoparticles. Thus, biological synthesis of the iron oxide nanoparticles is one of the most suitable, reproducible methods where particle size, surface charge, surface functionalization can be easily controlled for their potential biomedical use as an antimicrobial, antioxidant and anticancer agent.

### Declaration of Competing Interest

The authors have no known conflicts of interest associated with this article.

### Acknowledgement

We are grateful to the Department of Pharmaceutical Sciences and Drug Research, Punjabi University, Patiala, Punjab.

### References

- Bhattacharjee, S., 2016. DLS and zeta potential – what they are and what they are not?. *J. Control Release* 235, 337–351.
- Blanco-Andujar, C., Ortega, D., Southern, P., Pankhurst, Q.A., Thanh, N.T., 2015. High performance multi-core iron oxide nanoparticles for magnetic hyperthermia: Microwave synthesis, and the role of core-to-core interactions. *Nanoscale* 7, 1768–1775.
- Blois, M.S., 1958. Antioxidant determinations by the use of a stable free radical. *Nature* 181, 1199–1200.
- Das, A.K., Marwal, A., Verma, R., 2014. Datura innoxia leaf extract mediated one step green synthesis and characterization of magnetite (Fe<sub>3</sub>O<sub>4</sub>) nanoparticles. *Res. Rev. J. Pharm. Anal.* 2, 21–24.
- Dorniani, D., Hussein, M.Z., Kura, A.U., Fakurazi, S., Shaari, A.H., Ahmad, Z., 2012. Preparation of Fe<sub>3</sub>O<sub>4</sub> magnetic nanoparticles coated with gallic acid for drug delivery. *Int. J. Nanomed.* 7, 5745–5756.
- Gupta, A.K., Gupta, M., 2005. Synthesis and surface engineering of iron oxide nanoparticles for biomedical application. *Biomaterials* 26, 3995–4021.
- Hariani, P.L., Faizal, M., Setiabudidaya, D., 2013. Synthesis and properties of Fe<sub>3</sub>O<sub>4</sub> nanoparticles by Co-precipitation method to removal procion dye. *Int. J. Environ. Sci.* 4, 336–340.
- Hoag, G.E., Collins, J.B., Holcomb, J.L., Hoag, J.R., Nadagouda, M. N., Varma, R.S., 2009. Degradation of bromothymol blue by 'greener' nano-scale zero-valent iron synthesized using tea polyphenols. *J. Mater. Chem.* 45, 8671–8677.
- Igwe, O.U., Nwamezie, F., 2018. Green synthesis of iron nanoparticles using flower extract of *Piliostigma thonningii* and antibacterial activity evaluation. *Chem. Int.* 4, 60–66.
- Ishikawa, T., Kondo, K., Kitajima, J., 2003. Water-soluble constituents of coriander. *Chem. Pharm. Bull.* 51, 32–39.
- Kamat, A., Pingulkar, K., Bhushan, B., Gholap, A.P., Thomas, P., 2003. Potential application of low dose gamma irradiation to improve the microbiological safety of fresh coriander leaves. *Food. Cont.* 14, 529–537.
- Kim, H., Moon, J.Y., Kim, H., Lee, D.S., Cho, M., Choi, H.K., Kim, Y.S., Mosaddik, A., Cho, S.K., 2010. Antioxidant and antiproliferative activities of mango (*Mangifera indica* L.) flesh and peel. *Food. Chem.* 121, 429–436.
- Mahdavi, M., Namvar, F., Ahmad, M.B., Mohamad, R., 2013. Green biosynthesis and characterization of magnetic iron oxide (Fe<sub>3</sub>O<sub>4</sub>) nanoparticles using seaweed (*Sargassum muticum*) aqueous extract. *Molecules* 18, 5954–5964.
- Majeed, M.I., Lu, Q., Yan, W., Li, Z., Hussain, I., Tahir, M.N., Tremel, W., Tan, W.B., 2013. Highly water-soluble magnetic iron oxide (Fe<sub>3</sub>O<sub>4</sub>) nanoparticles for drug delivery: Enhanced in vitro therapeutic efficacy of doxorubicin and mion conjugates. *J. Mater. Chem. B* 22, 2874–2884.
- Mulvaney, P., 1996. Surface plasmon spectroscopy of nanosized metal particles. *Langmuir* 12, 788–800.
- Nadagouda, M.N., Castle, A.B., Murdock, R.C., Hussain, S.M., Varma, R.S., 2010. In vitro biocompatibility of nanoscale zero-valent iron particles (NZVI) synthesized using tea polyphenols. *Green. Chem.* 12, 114–122.
- Nambiar, V.S., Daniel, M., Guin, P., 2010. Characterization of polyphenols from coriander leaves (*Coriandrum sativum*), red amaranthus (*A. paniculatus*) and green amaranthus (*A. frumentaceus*) using paper chromatography: and their health implications. *J. Herb. Med. Toxicol.* 4, 173–177.
- Nielsen, O.H., Soendergaard, C., Vikner, M.E., Weiss, G., 2018. Rational management of iron-deficiency anaemia in inflammatory bowel disease. *J. Nutr.* 10.
- Njagi, E.C., Huang, H., Stafford, L., Genuino, H., Galindo, H.M., Collins, J.B., Hoag, G.E., Suib, S.L., 2010. Biosynthesis of iron and silver nanoparticles at room temperature using aqueous sorghum bran extracts. *Langmuir* 27, 264–271.
- Prasad, K.S., Gandhi, P., Selvaraj, K., 2014. Synthesis of green nano iron particles (GnIP) and their application in adsorptive removal of As (III) and As (V) from aqueous solution. *Appl. Surf. Sci.* 317, 1052–1059.
- Rodger, M., Sheppard, D., Gandara, E., Tinmouth, A., 2015. Haematological problems in obstetrics. *Best. Pract. Res. Clin. Obstet. Gynaecol.* 29, 671–684.
- Shahwan, T., Abu, Sirriah, S., Nairat, M., Boyaci, E., Eroğlu, A.E., Scott, T.B., Hallam, K.R., 2011. Green synthesis of iron nanoparticles and their application as a Fenton-like catalyst for the degradation of aqueous cationic and anionic dyes. *Chem. Eng.* 172, 258–266.
- Shi, S.F., Jia, J.F., Guo, X.F., Zhao, Y.P., Chen, D.S., Guo, Y.Y., 2012. Biocompatibility of chitosan-coated iron oxide nanoparticles with osteoblast cells. *Int. J. Nanomed.* 7, 5593–5602.
- Sood, R., Chopra, D.S., 2018. Optimization of reaction conditions to fabricate *Ocimum sanctum* synthesized silver nanoparticles and its application to nano-gel systems for burn wounds. *Mater. Sci. Eng. C.* 92, 575–589.
- Tudisco, C., Cambria, T.M., Sinatra, F., Bertani, F., Alba, A., Giuffrida, E.A., Saccone, S., Fantechi, E., 2015. Multifunctional magnetic nanoparticles for enhanced intracellular drug transport. *J. Mater. Chem. B.* 20, 4134–4145.
- Turakhia, B., Chapla, K., Turakhia, P., 2017. Green synthesis of Zero valent iron nanoparticles from *Coriandrum sativum* and its application in reduction chemical oxygen demand and biological oxygen demand in wastewater. *South-Asian J. Multidiscip. Stud.* 5, 132–139.
- Turakhia, B., Turakhia, P., Shah, S., 2018. Green synthesis of zero valent iron nanoparticles from *Spinacia oleracea* (spinach) and its application in wastewater treatment. *J. Adv. Res.* 5, 46–51.
- Wang, Z., Fang, C., Megharaj, M., 2014. Characterization of iron-polyphenol nanoparticles synthesized by three plant extracts and their Fenton oxidation of azo dye. *ACS Sustain. Chem. Eng.* 2, 1022–1025.
- Zhu, J., Wang, J., Wang, X., Zhu, J., Yang, Y., Tian, J., Cui, W., Ge, C., 2015. Facile synthesis of magnetic core-shell nanocomposites for MRI and CT bimodal imaging. *J. Mater. Chem. B.* 3, 6905–6910.
- Zhuang, L., Zhang, W., Zhao, Y., Shen, H., Lin, H., Liang, J., 2014. Preparation and characterization of Fe<sub>3</sub>O<sub>4</sub> particles with novel Nano sheets morphology and magneto chromatic property by a modified solvothermal method. *Sci. Rep.* 5, 21–26.